Tetrahedron 66 (2010) 6725–6732

Contents lists available at ScienceDirect

Tetrahedron

journal homepage: www.elsevier.com/locate/tet

Synthesis of dihydroxyoligophenylenes containing π-deficient or π-excess hetero-aromatic rings and their solvatochromic behavior

Isao Yamaguchi *, Kenji Seo, Yukari Kawashima

Department of Material Science, Faculty of Science and Engineering, Shimane University, 1060 Nishikawatsu, Matsue 690-8504, Japan

ARTICLE INFO

Article history:
Received 18 May 2010
Received in revised form
25 June 2010
Accepted 28 June 2010
Available online 3 July 2010

Keywords:
Dihydroxyoligophenylene
Suzuki coupling
Hetero-aromatic ring
Photoluminescence
Solvatochromism

ABSTRACT

Dihydroxyoligophenylenes (**HO-ArPh(*m*)-OH**s) with 9,9-dihexyl-2,7-fluorene (Ar=Flu), 2,5-dioctyloxy-1,4-benzene (Ar=Dob), pyridine (Ar=Py), or thiophene (Ar=Th) rings were synthesized by the Suzuki coupling reaction. Absorption maxima (λ_{max}) of **HO-ArPh(*m*)-OH**s shifted progressively toward long wavelengths due to the expansion of the π-conjugation system with an increase in the number of benzene rings. Deprotonation of the OH groups of **HO-ArPh(*m*)-OH**s by treatment with NaH caused a bathochromic shift of λ_{max}. The bathochromic shift of the deprotonated species increased with the donor numbers (DNs) of the solvents. The emission peak positions of **NaO-ArPh(*m*)-ONa**s depended on the DNs of the solvents; therefore, the emission color could be tuned by changing the solvent.

1. Introduction

Oligo(*p*-phenylene)s (OPPs) are an important class of π-conjugated oligomers because they are useful as luminophores for light-emitting materials,[1–6] as semiconductors for field-effect transistors,[7] as rigid-rod cores for liquid crystalline materials,[8–10] and as amphiphilic materials for biological applications.[11–15] A systematic investigation of OPPs containing various substituents has revealed that the chemical and physical properties of substituted OPPs depend on the type of substituents employed. Recently, we have reported OPPs with an OH group located at one end and at both ends, namely, **OPP(*n*)-OH**s (where *n* is the number of benzene rings) and **HO-OPP(3)-OH**, respectively.[16] The OPPs exhibited significant solvatochromism; the deprotonation of the OH groups of **OPP(*n*)-OH**s and **HO-OPP(3)-OH**, when treated with NaH, caused a bathochromic shift of λ_{max} that increased with the donor numbers (DNs) of the solvents. Furthermore, the emission peak positions of **OPP(*n*)-ONa**s and **NaO-OPP(3)-ONa** depended on the DNs of the solvents; therefore, the emission color could be tuned by changing the solvent. However, we were unable to investigate the optical properties of **OPP(*n*)-OH** and **HO-OPP(*n*)-OH** ($n>4$) in detail because of their low solubility. In this study, to obtain soluble dihydroxyoligophenylenes, namely, **HO-ArPh(*m*)-OH**s (where *m* is the number of benzene rings), with a longer *p*-phenylene group ($m\geq4$), 9,9-dihexyl-2,7-fluorene (Ar=Flu) and 2,5-dioctyloxy-1,4-benzene (Ar=Dob) units were used as building blocks, and 9,9-dihexylfluorene-2,7-diboronic acid bis(1,3-propanediol) ester (**1**) and 2,5-dioctyloxy-1,4-benzenediboronic acid (**2**) were reacted with **Br-OPP(*n*)-OH**s ($n=1$, 2, and 3).

The abovementioned solvatochromism exhibited by **OPP(*n*)-ONa**s and **NaO-OPP(3)-ONa** was attributed to an intramolecular charge shift from the sodium phenoxy group(s) to the adjacent rings.[5] In this study, in addition to soluble **HO-ArPh(*m*)-OH**s (Ar=Flu and Doc), **HO-ArPh(*m*)-OH**s with a π-deficient pyridine (Ar=Py) ring or a π-excess thiophene (Ar=Th) ring were synthesized by the Suzuki coupling reaction. The presence of π-deficient or π-excess aromatic rings in **HO-ArPh(*m*)-OH**s would significantly affect the optical properties of **HO-ArPh(*m*)-OH**s because the charge shift from the sodium phenoxide groups to the adjacent rings depends on the electronic properties of the accepting site (Ar). To the best of our knowledge, however, no systematic studies have been conducted on the optical properties of **HO-ArPh(*m*)-OH**s with π-deficient or π-excess hetero-aromatic rings. Elucidation of the optical properties of **HO-ArPh(*m*)-OH**s before and after the deprotonation of the OH groups will lead to a better understanding of the intramolecular charge shift in the π-conjugated oligoarylenes and toward the development of new functional materials. Additionally, **HO-ArPh(*m*)-OH**s can be useful starting materials for highly luminescent and thermally stable polymers.

Herein, we report the synthesis of **HO-ArPh(*m*)-OH**s with a longer *p*-phenylene group ($m\geq4$) and π-deficient or π-excess hetero-aromatic rings as well as their optical properties before and after the deprotonation of the OH groups.

* Corresponding author. E-mail address: iyamaguchi@riko.shimane-u.ac.jp (I. Yamaguchi).

0040-4020/$ – see front matter © 2010 Elsevier Ltd. All rights reserved.
doi:10.1016/j.tet.2010.06.087

2. Results and discussion

2.1. Synthesis

The reaction of **1** with 4-bromophenol, 4-bromo-4′-hydroxybiphenyl, and 4-bromo-4″-methoxy[1,1′;4′,1″]terphenyl (**Br-OPP(3)-OMe**) in a 1:2 molar ratio afforded **HO-FluPh(4)-OH**, **HO-FluPh(6)-OH**, and **MeO-FluPh(8)-OMe** in 59%, 73%, and 56% yields, respectively (Scheme 1a and b). The Suzuki coupling reaction of **1** with 4-bromo-4″-hydroxy[1,1′;4′,1″]terphenyl (**Br-OPP(3)-OH**) was not used for the synthesis of **HO-FluPh(8)-OH**. This is because the solubility of **HO-FluPh(8)-OH** in organic solvents was low, and therefore, it could not be purified by column chromatography. Instead of the above method, the reaction between 4-bromo-4″-methoxy[1,1′;4′,1″]terphenyl **Br-OPP(3)-OMe** and **1** and deprotection of the OMe groups was used for the synthesis of **HO-FluPh(8)-OH** (Scheme 1b). **HO-DobPh(*m*)-OH**s were obtained by the reaction of **2** with **Br-OPP(*n*)-OH**s (n=1, 2, and 3) in 55%, 63%, and 51% yields, respectively (Scheme 1c). In order to compare the chemical properties with **HO-DobPh(5)-OH**, **EtO-DobPh(5)-OEt** was synthesized by the hydrolysis of **HO-DobPh(5)-OH** with EtOH. **HO-AntPh(2)-OH** with an anthracene (Ar=Ant) luminophore was synthesized by the reaction of 4-hydroxyphenylboronic acid with 9,10-dibromoanthracene (Scheme 1d).

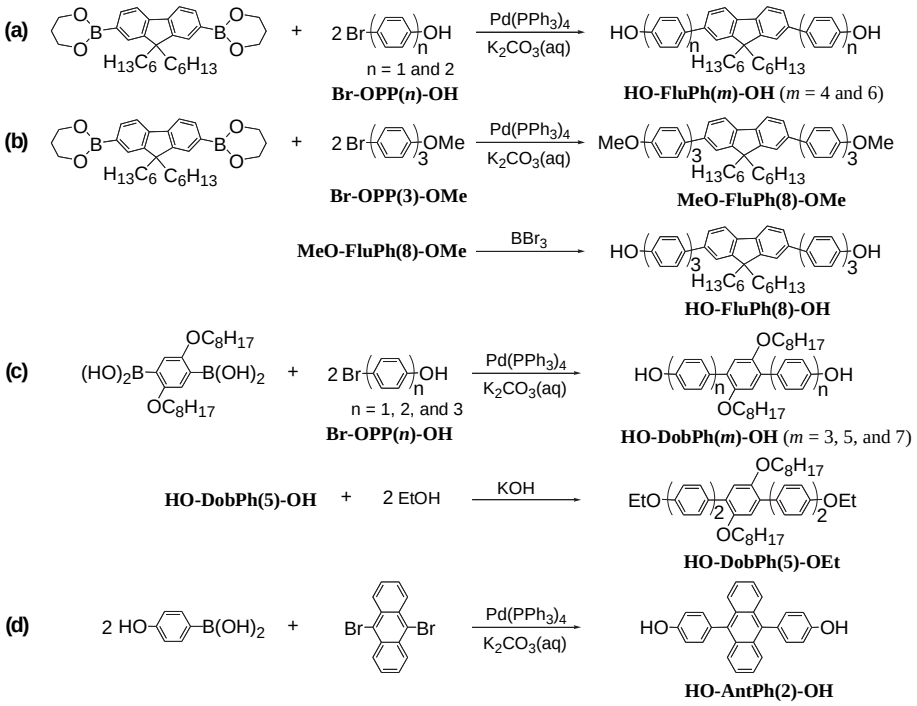

Scheme 1. Synthesis of soluble OPPs with hydroxyl groups at both ends.

Dihydroxyoligoarylenes bearing a central heterocyclic aromatic ring **HO-ArPh(*m*)-OH**s (Ar=Py and Th) were synthesized by the Suzuki coupling reactions shown in Scheme 2. The Suzuki coupling reaction of 4-bromophenol with thiophene-2,5-boronic acid in a 2:1 molar ratio did not yield an expected 2:1 coupling product but instead yielded a 1:1 coupling product (**HO-ThPh(2)**); the reason for this result is not entirely clear. However, the reaction of 4-bromo-4-hydroxybiphenyl with thiophene-2,5-diboronic acid in a 2:1 molar ratio yielded a 2:1 coupling product (**HO-ThPh(4)-OH**), as expected (Scheme 2b).

The structures of the newly synthesized compounds were determined by ^{1}H and ^{13}C NMR spectroscopy and elemental analysis. **OPP(5)-OH**, which consisted of five benzene rings, showed considerably low solubility in polar organic solvents.[16] Despite the larger number of benzene rings in **HO-FluPh(6)-OH** and **HO-DobPh(5)-OH** than in **OPP(5)-OH**, **HO-FluPh(6)-OH** and **HO-DobPh(5)-OH** showed good solubility in organic solvents because of the presence of the long alkyl chains. They were soluble in polar organic solvents such as 1,4-dioxane, *N*,*N*-dimethylformamide (DMF), and dimethyl sulfoxide (DMSO) as well as in less polar organic solvents such as dichloromethane and toluene. However, **HO-FluPh(8)-OH** and **HO-DobPh(7)-OH** were completely soluble in chloroform and dichloromethane but sparingly soluble in DMF and DMSO. **HO-PyPh(2)-OH** was soluble in DMF and DMSO but insoluble in dichloromethane and chloroform because of the presence of a hydrophilic pyridine ring.

The melting points of **HO-FluPh(*m*)-OH**s and **HO-DobPh(*m*)-OH**s increased as the number of the benzene ring (m) increased.

2.2. IR and NMR spectra

The main features of the IR spectra of **HO-FluPh(*m*)-OH**s were identical: the absorption peaks resulting from O–H stretching, presence of a phenyl ring, and out-of-plane C–H bending vibrations

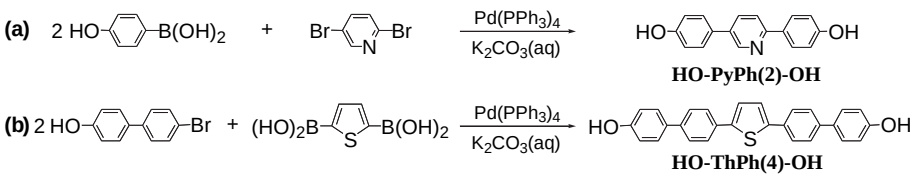

Scheme 2. Synthesis of **HO-ArPh(*m*)-OH**s with a central aromatic heterocycle.

of *p*-phenylene were observed at approximately 3440 cm^{-1}, 1250 cm^{-1}, and 815 cm^{-1}, respectively. Similarly, the main features of the IR spectra of **HO-DobPh(*m*)-OH**s were identical: the absorption peaks resulting from O–H stretching, presence of a phenyl ring, and out-of-plane C–H bending vibrations of *p*-phenylene were observed at approximately 3350 cm^{-1}, 1250 cm^{-1}, and 820 cm^{-1}, respectively.

Deprotonation of the OH groups of **HO-ArPh(*m*)-OH**s was carried out by treating them with an excess amount of NaH in DMSO-d_6. The disappearance of the signal ascribes to OH group from the ^{1}H NMR spectra of solutions of **HO-ArPh(*m*)-OH**s, except for **HO-FluPh(8)-OH** and **HO-DobPh(7)-OH**, and NaH indicated that the deprotonation proceeded quantitatively. The signals ascribed to particular protons of **NaO-ArPh(*m*)-ONa**s (Ar=Flu and Dob) shifted to higher magnetic fields than those of **HO-ArPh(*m*)-OH**s (Ar=Flu and Dob). These chemical shifts increase with decreasing the distance of the protons from the ONa group; therefore, they are largest in the case of protons adjacent to the ONa groups. These observations can be attributed to the electron-donating effect of the ONa groups. These data indicated the possibility of the occurrence of a charge shift from the phenolate groups to the adjacent rings in the deprotonated species. Such a charge shift in **NaO-ArPh(*m*)-ONa**s may significantly affect their optical properties. The ^{1}H NMR chemical shifts (δ_1 and δ_2) of protons adjacent to the OH groups in **HO-ArPh(*m*)-OH**s and the ONa groups in **NaO-ArPh(*m*)-ONa**s and their differences ($\Delta\delta=\delta_1-\delta_2$) are summarized in Table 1. The $\Delta\delta$ values depended on the electron density of the central ring in **NaO-ArPh(*m*)-ONa**s. That is, the $\Delta\delta$ values of **NaO-ArPh(*m*)-ONa**s (Ar=Flu and Dob) were smaller than those of **OPP(*n*)-ONa**s because of the presence of the electron-donating alkyl groups on the central phenylene ring, whereas, the $\Delta\delta$ value of **NaO-PyPh(2)-ONa** ($\Delta\delta$=0.90) was larger than those of **NaO-ArPh(*m*)-ONa**s (Ar=Flu and Dob) ($\Delta\delta$=0.64–0.80). This difference was apparently due to the presence of the central electron-accepting pyridine ring that easily induced the shift in charge from the phenolate groups to the adjacent rings in the deprotonated species.

Table 1
^{1}H NMR chemical shift

	δ_1		δ_2	$\Delta\delta=\delta_1-\delta_2$
HO-FluPh(4)-OH	6.94	**NaO-FluPh(4)-ONa**	6.14	0.80
HO-FluPh(6)-OH	6.88	**NaO-FluPh(6)-ONa**	6.08	0.80
HO-FluPh(8)-OH	6.88	**NaO-FluPh(8)-ONa**	6.08	0.80
HO-DobPh(5)-OH	6.86	**NaO-DobPh(5)-ONa**	6.22	0.64
HO-AntPh(2)-OH	7.03	**NaO-AntPh(2)-ONa**	6.24	0.79
HO-PyPh(2)-OH	6.88	**NaO-PyPh(2)-ONa**	5.98	0.90
HO-ThPh(4)-OH	6.86	**NaO-ThPh(4)-ONa**	6.05	0.81

The ^{13}C NMR peaks corresponding to the phenyl carbons adjacent to the ONa groups were observed at higher magnetic field positions (δ=117.2 and 126.8) than those adjacent to the OH groups of **HO-PyPh(2)-OH** (δ=118.9 and 127.7). These observations are attributed to the electron-donating effect of the ONa groups in **NaO-PyPh(2)-ONa**.

2.3. UV–vis absorption and solvatochromism

Figure 1 shows the UV–vis spectra of **HO-ArPh(*m*)-OH**s (Ar=Flu and Dob) in DMSO. The UV–vis data of **HO-ArPh(*m*)-OH**s (Ar=Flu and Dob) and their deprotonated species are summarized in Table 2. The absorption maxima (λ_{max}) of **HO-ArPh(*m*)-OH**s (Ar=Flu and Dob) shifted progressively toward longer wavelengths because of the expansion of the π-conjugation system as the number of benzene rings (*m*) increased.

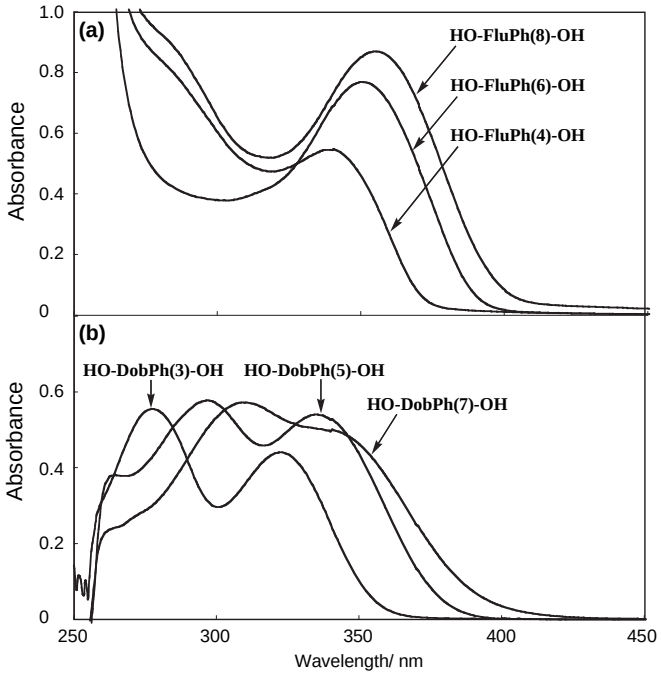

Figure 1. UV–vis spectra of **HO-ArPh(*m*)-OH**s (Ar=Flu (a) and Dob (b)) in DMSO.

The treatment of the DMSO solutions of **HO-ArPh(*m*)-OH**s (Ar=Flu and Dob) with NaH causes bathochromic shift of λ_{max} by approximately 50–80 nm. The formation of **NaO-ArPh(*m*)-ONa**s (Ar=Flu and Dob) was mainly responsible for the shift of λ_{max} toward a longer wavelength. Similar solvatochromic behavior was observed in the case of **OPP(*n*)-OH**s (*n*=3, 4, and 5) and their deprotonated species reported earlier.[16] To prove that these observations were due to the deprotonation of the OH groups after treatment with NaH, we confirmed that there was no change in the absorption spectra of **MeO-FluPh(8)-OMe** and **EtO-DobPh(5)-OEt** after the addition of NaH.

Bathochromic shift attributable to deprotonation depends on the donor number (DN) of the solvents. As shown in Figures 2 and 3, the λ_{max} values of **HO-ArPh(*m*)-OH**s (Ar=Flu and Dob) and their deprotonated species shifted to longer wavelengths as the DNs of the solvents increased.

In contrast to the small bathochromic shift of **HO-ArPh(*m*)-OH**s (Ar=Flu and Dob) with an increase in the DNs of the solvents, the λ_{max} values of the deprotonated species were larger than those of **HO-ArPh(*m*)-OH**s (Ar=Flu and Dob). For example, the λ_{max} value of **NaO-FluPh(4)-ONa** moves from 332 nm in CH_2Cl_2 (DN=0) to 414 nm in DMSO (DN=29.8) through to a value of 373 nm in THF (DN=20.0). The large $\Delta\lambda$ value can be attributed to the fact that solvents with a high DN solvate effectively with Na^+ to stabilize the deprotonated species in the solutions. Similar solvatochromic behavior was observed in the case of **OPP(*n*)-OH**s (*n*=4 and 5) and **OPP(*n*)-ONa**s (*n*=4 and 5) reported earlier.[5] The λ_{max} and $\Delta\lambda$ values of **NaO-FluPh(4)-ONa** were larger than those of **NaO-DobPh(5)-ONa** despite the smaller number of benzene rings in **NaO-FluPh(4)-ONa** than in **NaO-DobPh(5)-ONa**. This was because of the reduced π-conjugation length in **NaO-DobPh(5)-ONa**, which was attributed to the bond twisting between dioctyloxybenzene and the adjacent benzene rings induced by the steric hindrance of the dioctyloxy groups. In CH_2Cl_2, 1,4-dioxane, and THF, the absorption positions of **NaO-FluPh(8)-ONa** and **NaO-DobPh(7)-ONa** were longer than those of **NaO-FluPh(6)-ONa** and **NaO-DobPh(5)-ONa** because of the larger number of benzene rings in **NaO-FluPh(8)-ONa** and **NaO-DobPh(7)-ONa**. However, in DMF and DMSO, the

Table 2
UV–vis data of **HO-FluPh(*m*)-OH**s and **HO-DobPh(*m*)-OH**s

Solvent	DN[b]	**HO-FluPh(*m*)-OH**,[a] nm			**NaO-FluPh(*m*)-ONa**,[a] nm			**HO-DobPh(*m*)-OH**,[a] nm			**NaO-DobPh(*m*)-ONa**,[a] nm		
		m=4	6	8	*m*=4	6	8	*m*=3	5	7	*m*=3	5	7
Dichloromethane	0	279 (4.91)	341 (4.98)	280 (4.79)	332	341 (4.71)	279 (4.63)	272 (4.74)	291 (4.76)	[c]	[c]	[c]	[c]
		332 (4.72)		349 (4.96)			349 (4.85)	320 (4.54)	322 (4.66)				
1,4-Dioxane	14.8	275 (4.72)	345 (4.94)	347 (4.83)	275 (4.85)	344 (4.69)	275 (4.86)	273 (4.73)	293 (4.77)	304 (4.92)	273 (4.71)	340 (4.52)	351 (4.60)
		333 (4.63)			333 (4.63)		351 (4.82)	318 (4.50)	330 (4.69)		320 (4.50)		
THF	20.0	278 (4.87)	344 (4.94)	277 (4.86)	373 (4.62)	346 (4.52)	270 (5.01)	275 (4.78)	294 (4.83)	290 (4.88)	275 (4.75)	351 (4.51)	361 (4.66)
		335 (4.77)		350 (4.84)			381 (4.79)	320 (4.50)	332 (4.78)	308 (4.56)	317 (4.48)		
DMF	26.6	275 (5.03)	347 (4.72)	353 (4.80)	409 (4.71)	391 (4.09)	394 (4.60)	278 (4.76)	296 (4.80)	341	371 (4.60)	390 (4.66)	375
		338 (4.79)						322 (4.62)	336 (4.89)				
DMSO	29.8	275 (4.95)	347 (4.66)	284 (4.95)	414 (4.91)	421 (4.94)	407 (4.89)	279 (4.75)	297 (4.46)	310	373 (4.58)	396 (4.35)	396
		341 (4.74)		355 (4.94)				323 (4.61)	335 (4.43				

[a] Concentration of solution was 1.0×10^{-5} M. log ε values are shown in the parenthesis.
[b] DN=donor number.
[c] Not measured due to low solubility.

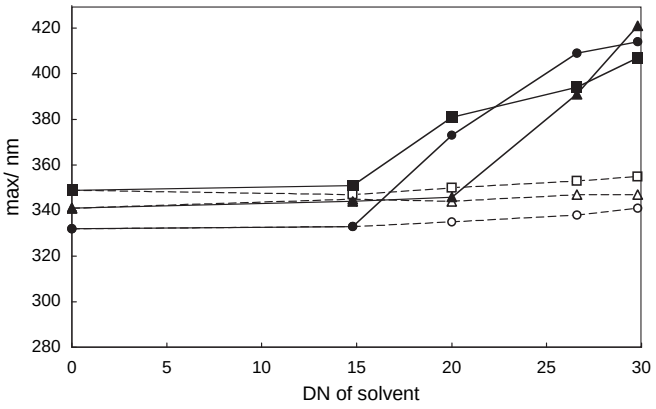

Figure 2. Dependence of λ_{max} of **HO-FluPh(*m*)-OH**s (*m*=4 (○), 6 (△), and 8 (□); dotted line) and their deprotonated species (*m*=4 (●), 6 (▲), and 8 (■); solid line) on the DNs of solvents. In the case that two absorption peaks were observed, the longer wavelength was adopted for the data point.

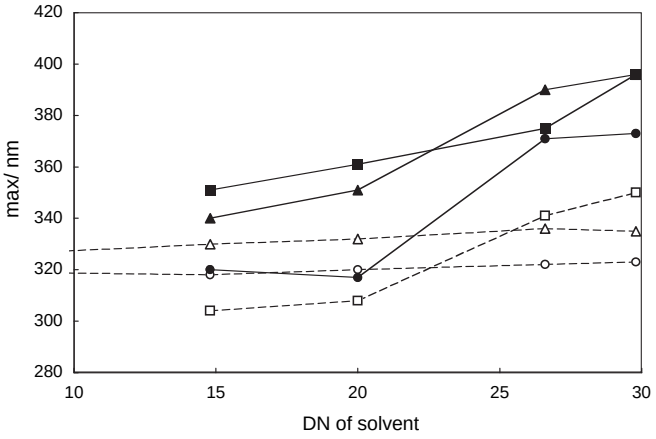

Figure 3. Dependence of λ_{max} of **HO-DobPh(*m*)-OH**s (*m*=3 (○), 5 (△), and 7 (□); dotted line) and their deprotonated species (*m*=4 (●), 6 (▲), and 8 (■); solid line) on the DNs of solvents. In the case that two absorption peaks were observed, the longer wavelength was adopted for the data point.

absorption positions of **NaO-FluPh(8)-ONa** and **NaO-DobPh(7)-ONa** were shorter than those of **NaO-FluPh(6)-ONa** and **NaO-DobPh(5)-ONa**. These observations are attributed to the low solubility of **HO-FluPh(8)-OH** and **HO-DobPh(7)-OH** in DMF and DMSO, which makes it difficult to form **NaO-FluPh(8)-ONa** and **NaO-DobPh(7)-ONa** by deprotonation of the OH groups with NaH. Approximate yields for **NaO-FluPh(8)-ONa** and **NaO-DobPh(5)-ONa**, estimated from the integration of the ^{1}H NMR peaks at δ_1 and δ_2, were 30% and 25%, respectively.

As mentioned above, the bathochromic shift in the λ_{max} of **HO-FluPh(*m*)-OH**s increased as the DNs of the solvents increased. In order to investigate the effect of pH of solvents on the optical properties of **HO-FluPh(*m*)-OH**s, the UV–vis measurements of **HO-FluPh(6)-OH** in the mixture of DMSO and aqueous buffer solutions (pH=1–10) were carried out. The UV–vis spectra of **HO-FluPh(6)-OH** in the solutions under pH of 7 showed a λ_{max} at approximately 330 nm, while those in the solutions above pH of 8 showed a λ_{max} at approximately 370 nm. The results that λ_{max} values of **HO-FluPh(6)-OH** in the basic solutions were larger than those in the acid solutions corresponded to the results that λ_{max} value of **NaO-FluPh(6)-ONa** was larger than that of **HO-FluPh(6)-OH** in solution.

UV–vis data of **HO-ArPh(*m*)-OH**s (Ar=Py and Th) and their deprotonated species are summarized in Table 3. A bathochromic shift caused by deprotonation was observed in the case of **HO-ArPh**

(***m***)-**OH**s (Ar=Py and Th). The $\Delta\lambda$ values of **NaO-PyPh(2)-ONa** in DMF and DMSO were larger than those of **NaO-FluPh(6)-ONa** despite the smaller number of benzene rings in **NaO-PyPh(2)-ONa** than in **NaO-FluPh(6)-ONa**. The larger bathochromic shift of **NaO-PyPh(2)-ONa** may be assumed to be caused by an effective shift in charge from the phenolate groups at both ends to the central electron-withdrawing pyridine ring. This assumption is in good agreement with the result that the ^{1}H NMR peak shifts of the protons adjacent to the ONa groups of **NaO-PyPh(2)-ONa** ($\Delta\delta$=0.90) produced by deprotonation were larger than those of **NaO-FluPh(6)-ONa** ($\Delta\delta$=0.80). The $\Delta\delta$ values of **NaO-ThPh(4)-ONa** in THF and DMSO were smaller than those of **NaO-PyPh(2)-ONa** despite the larger number of benzene rings in **NaO-ThPh(4)-ONa**. This is because of the presence of the central π-rich thiophene ring in **NaO-ThPh(4)-ONa**, which makes the shift in charge difficult from the phenolate groups to the adjacent rings in the deprotonated species.

The quantum yields of the PLs of the THF solutions of **NaO-FluPh(*m*)-ONa**s (*m*=4, 6, and 8) were 16%, 9%, and 9%, respectively, while those of **HO-DobPh(*m*)-OH**s (*m*=3, 5, and 7) were 12%, 10%, and 11%, respectively. The fact that the quantum yields of the PLs of **NaO-ArPh(*m*)-ONa**s are lower than those of **HO-ArPh(*m*)-OH**s is attributed to the intramolecular charge shift (ICT) in **NaO-ArPh(*m*)-ONa**s. It has been reported that the ICT in π-conjugated molecules reduces their PL emission efficiencies.[19]

Figures 5 and 6 show the dependence of the emission peak positions of **HO-ArPh(*m*)-OH**s (Ar=Flu and Dob) and their deprotonated species on the DNs of the solvents. Thus, by alternating solvents such as CH_2Cl_2 and 1,4-dioxane, which have small DN values, and those such as DMF and DMSO, which have large DN values, it is observed that the emission peak positions of **HO-ArPh(*m*)-OH**s (Ar=Flu and Dob) shift only by 3–10 nm. However, a significantly large shift in the

Table 3
UV–vis data of **HO-AntPh(2)-OH**, **HO-PyPh(2)-OH**, **HO-ThPh(4)-OH**, and their deprotonated species

Solvent	DN[b]	Absorption,[a] nm					
		HO-AntPh(2)-OH	**NaO-AntPh(2)-ONa**	**HO-PyPh(2)-OH**	**NaO-PyPh(2)-ONa**	**HO-ThPh(4)-OH**	**NaO-ThPh(4)-ONa**
Dichloromethane	0	339, 358, 376, 397	348	[c]	[c]	299	278, 351
1,4-Dioxane	14.8	340, 358, 376, 396	340, 358, 376, 391	[c]	[c]	289	269, 355
THF	20.0	342, 358, 376, 396	358, 378, 397, 433	278	273, 348	301	271, 369
DMF	26.6	342, 360, 378, 398	285, 327, 375, 474	283, 328	293, 389	314	403
DMSO	29.8	342, 361, 380, 400	294, 334, 376, 485	322	404, 487	321	399, 479

[a] Concentration of solution was 1.0×10^{-5} M.
[b] DN=donor number.
[c] Not measured due to low solubility.

2.4. Photoluminescence

It has been reported that OPPs exhibit photoluminescence (PL) with a high quantum yield.[17,18] **HO-ArPh(*m*)-OH**s and their deprotonated species are photoluminescent in solution. The PL data are summarized in Tables 4 and 5.

emission peaks of **NaO-ArPh(*m*)-ONa**s (Ar=Flu and Dob) occurred as the DNs of the solvents increased. These observations are comparable to the results that λ_{max} of **NaO-ArPh(*m*)-ONa**s (Ar=Flu and Dob) in solution shifts to a longer wavelength than that of **HO-ArPh(*m*)-OH**s (Ar=Flu and Dob) with an increase in the DNs of the solvents. The remarkable solvatochromic shift of the PL peak position of **NaO-ArPh**

Table 4
PL data of **HO-FluPh(*m*)-OH**s and **HO-DobPh(*m*)-OH**s

Solvent	DN[b]	**HO-FluPh(*m*)-OH**,[a] nm			**NaO-FluPh(*m*)-ONa**,[a] nm			**HO-DobPh(*m*)-OH**,[a] nm			**NaO-DobPh(*m*)-ONa**,[a] nm		
		m=4	6	8	*m*=4	6	8	*m*=3	5	7	*m*=3	5	7
Dichloromethane	0	369, 386 (329)	392, 408 (341)	401, 413[d] (348)	368, 385 (330)	392 (340)	403 (348)	384 (328)	404 (336)	[c]	[c]	[c]	[c]
1,4-dioxane	14.8	370, 388 (339)	396, 410 (345)	398, 413[d] (347)	370, 389 (336)	396 (341)	399, 484 (350)	383 (327)	403 (337)	409 (341)	385 (327)	458 (358)	429 (334)
THF	20.0	372, 390 (341)	395, 410 (344)	401, 415[d] (349)	451 (373)	401, 507 (344)	534 (381)	381 (329)	402 (338)	408 (342)	382 (328)	484 (362)	510 (381)
DMF	26.6	377, 394 (343)	398, 411 (348)	403, 420[d] (353)	495 (400)	534, 538 (415)	518 (393)	386 (330)	405 (341)	413 (344)	447 (373)	548 (379)	511 (381)
DMSO	29.8	379, 396 (345)	401, 415 (347)	406, 425[d] (354)	492 (402)	555 (420)	526 (404)	387 (331)	408 (343)	415 (347)	451 (372)	552 (382)	510 (382)

[a] Concentration of solution was 1.0×10^{-6} M. Excitation wavelength was shown in parenthesis.
[b] DN=donor number.
[c] Not measured due to low solubility.
[d] Shoulder peak.

The quantum yields of the PLs of the THF solutions of **HO-FluPh (*m*)-OH**s (*m*=4, 6, and 8) were 41%, 19%, and 34%, respectively, while those of **HO-DobPh(*m*)-OH**s (*m*=3, 5, and 7) were 36%, 34%, and 34%, respectively. The emission peak positions of **HO-ArPh(*m*)-OH**s and their deprotonated species depended on the DNs of the solvents; therefore, the emission color can be tuned by changing the solvent. For example, **NaO-DobPh(5)-ONa** exhibited purple, blue, and yellow emissions after it was irradiated with UV light in

(***m***)-**ONa**s (Ar=Flu and Dob) appeared to be due to the charge shift from the phenolate group to the adjacent rings. In addition to the charge shift effect, a large amount of stabilization energy produced by the solvation of **NaO-ArPh(*m*)-ONa**s (Ar=Flu and Dob) may contribute to the solvatochromic red shift as the DNs of the solvents increase. There was no change in the PL spectra of **MeO-FluPh(8)-OMe** and **EtO-DobPh(5)-OEt** after the addition of NaH, which suggested that the solvatochromism in **NaO-ArPh(*m*)-ONa**s (Ar=Flu and Dob)

Table 5
PL data of **HO-ArPh(*m*)-OH**s (Ar=Ant, Py, and Th) and their deprotonated species

Solvent	DN[b]	Photoluminescence,[a] nm					
		HO-AntPh(2)-OH	**NaO-AntPh(2)-ONa**	**HO-PyPh(2)-OH**	**NaO-PyPh(2)-ONa**	**HO-ThPh(4)-OH**	**NaO-ThPh(4)-ONa**
Dichloromethane	0	421, 437[d] (396)	401, 420[d] (348)	[c]	[c]	401, 418,[d] 445[d] (348)	401, 419,[d] 447[d] (351)
1,4-Dioxane	14.8	423, 441[d] (396)	401, 418[d] (360)	[c]	[c]	358,[d] 375, 393[d] (328)	443 (366)
THF	20.0	424, 443[d] (395)	401, 415, 509 (360)	375, 389[d] (328)	430 (367)	363,[d] 377, 398[d] (328)	476 (372)
DMF	26.6	433 (397)	526 (398)	386, 401 (329)	481 (392)	387 (328)	531 (399)
DMSO	29.8	436 (399)	532 (401)	383 (328)	486 (394)	391 (329)	532 (399)

[a] Concentration of solution was 1.0×10^{-6} M. Excitation wavelength was shown in parenthesis.
[b] DN=donor number.
[c] Not measured due to low solubility.
[d] Shoulder peak.

Figure 4. Photographs of **NaO-DobPh(5)-ONa** when it was irradiated with UV light in CH_2Cl_2 (DN=0), THF (DN=20.0), and DMSO (DN=29.8).

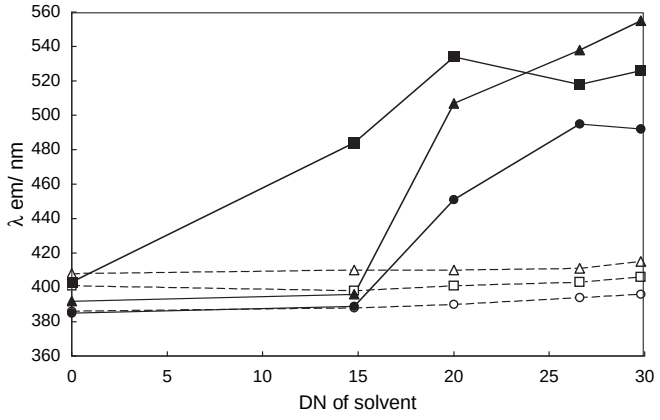

Figure 5. Dependence of PL peak position of **HO-FluPh(*m*)-OH**s (*m*=4 (○), 6 (△), and 8 (□); dotted line) and their deprotonated species (*m*=4 (●), 6 (▲), and 8 (■); solid line) on the DNs of solvents. In the case that two PL peaks were observed, the longer wavelength was adopted for the data point.

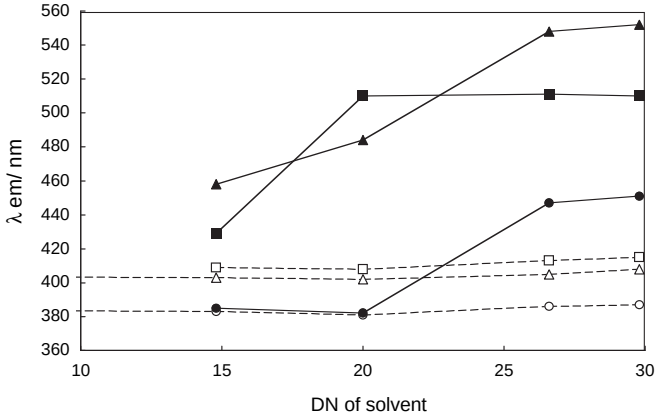

Figure 6. Dependence of PL peak position of **HO-DobPh(*m*)-OH**s (*m*=3 (○), 5 (△), and 7 (□); dotted line) and their deprotonated species (*m*=4 (●), 6 (▲), and 8 (■); solid line) on the DNs of solvents.

was attributed to the deprotonation of the OH group after treatment with NaH.

In DMF and DMSO, the PL peak positions of **NaO-FluPh(8)-ONa** and **NaO-DobPh(7)-ONa** were shorter than those of **NaO-FluPh(6)-ONa** and **NaO-DobPh(5)-ONa** despite the larger number of benzene rings in **NaO-FluPh(8)-ONa** and **NaO-DobPh(7)-ONa** than in **NaO-FluPh(6)-ONa** and **NaO-DobPh(5)-ONa**. These results are comparable to those that suggest λ_{max} positions of **NaO-FluPh(8)-ONa** and **NaO-DobPh(7)-ONa** were lower than those of **NaO-FluPh(6)-ONa** and **NaO-DobPh(5)-ONa**.

The PL peak position of **HO-FluPh(6)-OH** in the solutions under pH of 7 was observed at 401 nm, while that in the solutions above pH of 8 was 536 nm. These wavelengths are comparable to those of the DMSO solutions of **HO-FluPh(6)-OH** and **NaO-FluPh(6)-ONa**, respectively.

Similar to the case of **HO-ArPh(*m*)-OH**s (Ar=Flu and Dob) and their deprotonated species, the emission peak positions of **HO-ArPh(*m*)-OH**s (Ar=Ant, Py, and Th) and their deprotonated species depended on the DNs of the solvents. The PL data are summarized in Table 5. The emission peak positions of **NaO-AntPh(2)-ONa** and **NaO-ThPh(4)-ONa** in the solvents with a high DN value (DMF and DMSO) were considerably higher than those in the solvents with a low DN value (CH_2Cl_2 and 1,4-dioxane). Quantum yields of the PLs of the THF solutions of **HO-ArPh(*m*)-OH**s (Ar=Ant, Py, and Th) were 8%, 4%, and 15%, respectively, while those of **NaO-ArPh(*m*)-ONa**s (Ar=Ant, Py, and Th) were 7%, 3%, and 7%, respectively. These results are comparable to the results that quantum yields of the PL of **HO-ArPh(*m*)-OH**s (Ar=Flu and Dob) were higher than those of **NaO-ArPh(*m*)-ONa**s (Ar=Flu and Dob).

3. Conclusions

A series of dihydroxyoligophenylenes, namely, **HO-ArPh(*m*)-OH**s, containing 9,9-dihexyl-2,7-fluorene (Ar=Flu), 2,5-dioctyloxy-1,4-benzene (Ar=Dob), pyridine (Ar=Py), or 2,5-thiophene (Ar=Th) rings were synthesized by the Suzuki coupling reaction. The alkyl groups of **HO-ArPh(*m*)-OH**s (Ar=Flu and Dob) contributed toward improving their solubility. The treatment of **HO-ArPh(*m*)-OH**s with a base produced the deprotonated species **NaO-ArPh(*m*)-ONa**s, whose absorption and PL peak positions in solution shifted toward longer wavelengths with an increase in the DNs of the solvents. The emission colors of the solutions of the deprotonated species could be tuned by changing the solvent. The optical properties of **NaO-ArPh(*m*)-ONa**s were significantly affected by the π-electron density in the central aromatic ring. From the results of this study, it can be concluded that new luminescent materials can be developed on the basis of the remarkable solvatochromic behavior of **NaO-ArPh(*m*)-ONa**s.

4. Experimental section

4.1. General

Solvents were dried, distilled, and stored under nitrogen. **Br-OPP(3)-OH**, **Br-OPP(3)-OMe**, and **2** were synthesized according to the literatures.[16,20] Other reagents were purchased and used without further purification. Reactions were carried out with standard Schlenk techniques under nitrogen.

IR and NMR spectra were recorded on a JASCO FT/IR-660 PLUS spectrophotometer and a JEOL AL-400 spectrometer, respectively. Elemental analysis was performed on a Yanagimoto MT-5 CHN corder. UV–vis and PL spectra were obtained by a JASCO V-560 spectrometer and a JASCO FP-6200 spectrofluorometer, respectively. Quantum yields were calculated by using a diluted ethanol solution of 7-dimethylamino-4-methylcoumarin as the standard.

4.2. Synthesis of HO-FluPh(4)-OH

4-Bromophenol (0.35 g, 2.0 mmol) and **1** (0.50 g, 1.0 mmol) were dissolved in 25 mL of dry THF under N_2. K_2CO_3(aq) (2.0 M, 10 mL; N_2 bubbled before use) and $Pd(PPh_3)_4$ (0.049 g, 0.042 mmol) were added to the solution. After the mixture was refluxed for 48 h, the solvent was removed under vacuum. The resulting solid was washed with water and hexane and dried under vacuum to give a light yellow solid, which was dissolved in methanol (150 mL). The solution was treated with 0.5 N HCl(aq) (25 mL) and neutralized with NaOH(aq) to give a precipitate from the solution. The precipitate was collected by filtration and dried in vacuo to give **HO-FluPh(4)-OH** as a white powder (0.31 g, 59%). ^{1}H NMR (400 MHz, $CDCl_3$): δ 7.73 (d, *J*=7.6 Hz, 2H), 7.56 (d, *J*=8.8 Hz, 4H), 7.49–7.53 (m, 4H), 6.94 (d, *J*=8.4 Hz, 4H), 4.80 (br, 2H), 2.01 (m, 4H), 1.06 (m, 12H), 0.75 (m, 10H). ^{13}C NMR (100 MHz, $CDCl_3$): δ 155.0, 151.6, 139.6, 139.5, 134.5, 132.2, 128.4, 125.6, 121.1, 119.8, 115.7, 55.2, 40.5, 31.5, 29.7, 23.8, 22.6, 14.0. IR (KBr, cm^{-1}): 3333 (OH), 3031, 2926, 2856, 1604, 1514, 1459, 1248, 1175, 817. Anal. Calcd for $C_{37}H_{42}O_2$: C, 85.67; H, 8.16. Found: C, 85.53; H, 7.83. Mp=119–121 °C.

4.3. Synthesis of HO-FluPh(6)-OH and MeO-FluPh(8)-OMe

HO-FluPh(6)-OH and **MeO-FluPh(8)-OMe** were synthesized by the reaction of **1** with **Br-OPP(2)-OH** and **Br-OPP(3)-OMe** analogously.

*4.3.1. Data of **HO-FluPh(6)-OH**.* Yield=73%. ^{1}H NMR (400 MHz, $CDCl_3$): δ 7.79 (d, *J*=8.0 Hz, 2H), 7.74 (d, *J*=8.4 Hz, 4H), 7.61–7.67 (m, 8H), 7.56 (d, *J*=8.4 Hz, 4H), 6.94 (d, *J*=8.4 Hz, 4H), 4.88 (s, 2H), 2.07 (m, 4H), 1.13 (m, 12H), 0.77 (m, 10H). ^{13}C NMR (100 MHz, $CDCl_3$): δ 155.2, 151.7, 140.1, 139.6, 133.6, 128.3, 127.5, 127.1, 125.9, 121.4, 115.7, 55.3, 40.5, 31.5, 29.7, 23.8, 22.6, 14.0. IR (KBr, cm^{-1}): 3442 (OH), 2926, 2854, 1603, 1458, 1257, 1024, 817. Anal. Calcd for $C_{49}H_{50}O_2$: C, 87.72; H, 7.51. Found: C, 87.53; H, 7.43. Mp=193–195 °C.

*4.3.2. Data of **MeO-FluPh(8)-OMe**.* Yield=56%. ^{1}H NMR (400 MHz, $CDCl_3$): δ 7.72–7.82 (m, 14H), 7.59–7.68 (m, 10H), 7.02 (d, *J*=8.4 Hz, 4H), 3.88 (s, 6H), 2.07 (m, 4H), 1.12 (m, 12H), 0.77 (m, 10H). ^{13}C NMR (100 MHz, $CDCl_3$): δ 159.3, 151.8, 140.6, 140.2, 139.8, 139.5, 139.0, 133.2, 128.1, 127.6, 127.5, 127.4, 127.2, 127.1, 126.0, 121.4, 120.1, 114.3, 55.38, 55.32, 40.5, 31.5, 29.7, 23.8, 22.6, 14.0. IR (KBr, cm^{-1}): 3031, 2925, 2855, 1607, 1510, 1459, 1248, 1175, 817. Anal. Calcd for $C_{63}H_{62}O_2$: C, 88.90; H, 7.34. Found: C, 88.61; H, 7.09. Mp=300–302 °C.

4.4. Synthesis of HO-FluPh(8)-OH

After BBr_3 (1 mL) was added to a dichloromethane solution (70 mL) of **MeO-FluPh(3)-OMe** (0.078 g, 0.091 mmol) under N_2, the solution was stirred at 20 °C for 24 h. To the solution was water (50 mL), the organic layer was extracted with dichloromethane and dried over sodium sulfonate. The solvent was removed by evaporation to give a white solid, which was washed with hexane. **HO-FluPh(8)-OH** was collected by filtration, dried in vacuo, and obtained as a white powder (0.042 g, 56%). ^{1}H NMR (400 MHz, $CDCl_3$): δ 7.72–7.82 (m, 14H), 7.63–7.67 (m, 8H), 7.56 (d, *J*=8.4 Hz, 4H), 6.94 (d, *J*=8.4 Hz, 4H), 4.82 (s, 2H), 2.07 (m, 4H), 1.09 (m, 12H), 0.77 (m, 10H). ^{13}C NMR (100 MHz, DMSO-d_6): δ 157.3, 151.4, 149.1, 148.0, 139.7, 139.3, 138.5, 137.4, 135.5, 130.3, 127.6, 127.2, 126.9, 126.4, 125.5, 120.9, 120.4, 115.8, 55.0, 32.1, 30.8, 28.9, 23.4, 21.9, 13.7. IR (KBr, cm^{-1}): 3426 (OH), 3029, 2926, 2856, 1604, 1514, 1489, 1459, 1251, 1176, 815. Anal. Calcd for $C_{61}H_{58}O_2$: C, 89.01; H, 7.10. Found: C, 88.79; H, 6.58. Mp=252–254 °C.

4.5. Synthesis of HO-DobPh(*m*)-OHs

HO-DobPh(*m*)-OHs were synthesized by the Suzuki coupling reaction of **2** with **Br-Ph(*n*)-OH**s (*n*=1, 2, and 3).

*4.5.1. Data of **HO-DobPh(3)-OH**.* Yield=55%. ^{1}H NMR (400 MHz, $CDCl_3$): δ 7.49 (d, *J*=8.4 Hz, 4H), 6.93 (s, 2H), 6.88 (d, *J*=8.4 Hz, 4H), 3.89 (t, *J*=6.0 Hz, 4H), 3.50 (s, 2H), 1.68 (m, 4H), 1.25–1.35 (m, 20H), 0.88 (t, *J*=6.8 Hz, 6H). ^{13}C NMR (100 MHz, DMSO-d_6): δ 156.4, 149.5,

130.3, 129.1, 128.6, 115.4, 114.7, 68.6, 31.2, 28.8, 28.64, 28.57, 25.5, 22.1, 14.0. IR (KBr, cm^{-1}): 3363 (OH), 2925, 2853, 1611, 1524, 1496, 1461, 1383, 1211, 1173, 1054, 831, 631. Anal. Calcd for $C_{34}H_{46}O_4$: C, 78.72; H, 8.94. Found: C, 78.48; H, 8.75. Mp=117–119 °C.

4.5.2. Data of ***HO-DobPh(5)-OH***. Yield=63%. ^{1}H NMR (400 MHz, $CDCl_3$): δ 7.69 (d, J=8.0 Hz, 4H), 7.61 (d, J=8.4 Hz, 4H), 7.56 (d, J=8.4 Hz, 4H), 7.05 (s, 2H), 6.94 (d, J=7.6 Hz, 4H), 4.73 (s, 2H), 3.96 (t, J=6.4 Hz, 4H), 1.72 (m, 4H), 1.27–1.39 (m, 20H), 0.87 (t, J=6.0 Hz, 6H). ^{13}C NMR (100 MHz, $CDCl_3$): δ 155.0, 150.4, 139.2, 136.8, 133.8, 130.3, 129.9, 128.3, 126.2, 116.2, 115.6, 69.6, 31.8, 29.4, 29.3, 26.1, 22.7, 14.1. IR (KBr, cm^{-1}): 3340 (OH), 3031, 2925, 2856, 1603, 1482, 1381, 1218, 820. Anal. Calcd for $C_{46}H_{54}O_4$: C, 82.35; H, 8.94. Found: C, 82.15; H, 8.70. Mp=211–213 °C.

4.5.3. Data of ***HO-DobPh(7)-OH***. Yield=51%. ^{1}H NMR (400 MHz, $CDCl_3$): δ 7.74–7.77 (m, 12H), 7.68 (d, J=8.4 Hz, 4H), 7.59 (d, J=6.4 Hz, 4H), 6.97 (d, J=8.8 Hz, 4H), 4.90 (s, 2H), 4.01 (t, J=6.4 Hz, 4H), 1.76 (m, 4H), 1.28–1.43 (m, 20H), 0.89 (t, J=6.8 Hz, 6H). ^{13}C NMR (100 MHz, DMSO-d_6): δ 149.8, 139.2, 131.8, 129.9, 128.5, 127.7, 127.6, 127.0, 126.9, 126.7, 125.9, 121.9, 115.8, 115.6, 68.8, 31.2, 28.8, 28.7, 28.6, 25.6, 22.1, 13.9. IR (KBr, cm^{-1}): 3371 (OH), 3030, 2925, 2854, 1610, 1594, 1485, 1380, 1258, 1208, 1111, 1003, 815. Anal. Calcd for $C_{58}H_{64}O_4$: C, 84.63; H, 7.59. Found: C, 84.90; H, 7.00. Mp=256–257 °C.

4.6. Synthesis of EtO-DobPh(5)-OEt

Ethyl iodide (0.20 mL, 120 mmol) was added dropwise to the EtOH solution (6 mL) of **HO-DobPh(5)-OH** (0.40 g, 0.60 mmol) and KOH (0.13 g, 2.8 mmol). After the solution was refluxed for 24 h, resulting precipitate was collected by filtration and washed with water and acetone. **EtO-DobPh(5)-OEt** was collected by filtration, dried in vacuo, and obtained as a white powder (0.34 g, 78%). ^{1}H NMR (400 MHz, $CDCl_3$): δ 7.68 (d, J=8.4 Hz, 4H), 7.61 (d, J=8.4 Hz, 4H), 7.61 (d, J=8.0 Hz, 4H), 7.04 (s, 2H), 6.99 (d, J=8.8 Hz, 4H), 4.10 (q, J=7.2 Hz, 4H), 3.95 (t, J=6.4 Hz, 4H), 1.72 (m, 4H), 1.47 (t, J=6.8 Hz, 6H), 1.24–1.29 (m, 20H), 0.86 (t, J=6.0 Hz, 6H). ^{13}C NMR (100 MHz, $CDCl_3$): δ 158.5, 150.4, 139.3, 136.7, 133.3, 130.3, 129.9, 128.0, 126.2, 116.1, 114.8, 69.6, 63.5, 31.8, 29.4, 29.3, 26.1, 22.7, 14.9, 14.1. IR (KBr, cm^{-1}): 3033, 2924, 2854, 1607, 1508, 1492, 1477, 1388, 1273, 1250, 1216, 1174, 1045, 921, 822, 802. Anal. Calcd for $C_{50}H_{62}O_4$: C, 82.60; H, 8.60. Found: C, 82.85; H, 8.08. Mp=168–170 °C.

4.7. Synthesis of HO-AntPh(2)-OH, HO-ThPh(4)-OH, and HO-PyPh(2)-OH

HO-AntPh(2)-OH, **HO-ThPh(4)-OH**, and **HO-PyPh(2)-OH** were synthesized using a procedure similar to that used for **HO-FluPh (4)-OH**.

4.7.1. Data of ***HO-AntPh(2)-OH***. Yield=10%. ^{1}H NMR (400 MHz, DMSO-d_6): δ 9.69 (s, 2H), 7.65 (dd, J=3.2 and 6.8 Hz, 4H), 7.40 (dd, J=3.2 and 6.8 Hz, 4H), 7.23 (d, J=8.4 Hz, 4H), 7.03 (d, J=8.4 Hz, 4H). ^{13}C NMR (100 MHz, DMSO-d_6): δ 156.9, 136.5, 132.0, 129.7, 128.3, 126.6, 125.1, 115.4. IR (KBr, cm^{-1}): 3359 (OH), 3031, 1659, 1604, 1510, 1438, 1384, 1233, 1172, 827, 768. Anal. Calcd for $C_{26}H_{18}O_2$: C, 86.16; H, 5.01. Found: C, 86.48; H, 5.11. Mp=310–312 °C.

4.7.2. Data of ***HO-ThPh(4)-OH***. Yield=42%. ^{1}H NMR (400 MHz, DMSO-d_6): δ 9.59 (s, 2H), 7.69 (d, J=8.4 Hz, 4H), 7.63 (d, J=8.4 Hz, 4H), 7.53 (d, J=8.0 Hz, 4H), 7.15 (t, J=4.4 Hz, 2H), 6.86 (d, J=8.4 Hz, 4H). ^{13}C NMR (100 MHz, DMSO-d_6): δ 143.1, 139.2, 132.9, 128.5, 127.5, 126.4, 125.8, 125.4, 123.4, 115.8. IR (KBr, cm^{-1}): 3418 (OH), 2925, 1604, 1491, 1450, 1378, 1256, 818, 696. Anal. Calcd for $C_{26}H_{20}O_2S$: C, 78.76; H, 5.08. Found: C, 78.84; H, 4.60. Mp=292–294 °C.

4.7.3. Data of ***HO-PyPh(2)-OH***. Yield=35%. ^{1}H NMR (400 MHz, DMSO-d_6): δ 9.73 (s, 1H), 9.66 (s, 1H), 8.83 (d, J=2.4 Hz, 1H), 8.01 (dd, J=2.4 and 4.0 Hz, 1H), 7.96 (d, J=8.8 Hz, 2H), 7.87 (d, J=8.4 Hz, 1H), 7.59 (d, J=8.4 Hz, 2H), 6.88 (t, J=8.4 Hz, 4H). ^{13}C NMR (100 MHz, DMSO-d_6): δ 158.4, 157.6, 153.9, 146.4, 134.1, 133.0, 129.2, 127.7, 118.9, 115.9, 115.5. IR (KBr, cm^{-1}): 3399 (OH), 1602, 1517, 1469, 1374, 1252, 1176, 821. Anal. Calcd for $C_{17}H_{13}NO_2$: C, 77.55; H, 4.98; N 5.32. Found: C, 77.93; H, 4.84; N, 5.00. Mp=352–354 °C.

References and notes

1. Era, M.; Tsutsui, T.; Saito, S. *Appl. Phys. Lett.* **1995**, *67*, 2436–2438.
2. Meghdadi, F.; Leising, G.; Fisher, W.; Stelzer, F. *Synth. Met.* **1996**, *76*, 113–115.
3. Kauffman, J. M.; Litak, P. T.; Novinski, J. A.; Kelly, C. J.; Ghiorghis, A.; Qin, Y. *J. Fluoresc.* **1995**, *5*, 295–305.
4. Wang, Y. Z.; Sun, R. G.; Meghdadi, F.; Leising, G.; Epstein, A. J. *Appl. Phys. Lett.* **1999**, *74*, 3613–3615.
5. Li, Z.-H.; Wong, M.-S.; Tao, Y.; D'Iorio, M. *J. Org. Chem.* **2004**, *69*, 921–927.
6. Ahn, K.-H.; Ryu, G. Y.; Youn, S.-W.; Shin, D.-M. *Mater. Sci. Eng., C* **2004**, *24*, 163–165.
7. Grundlach, D. J.; Lin, Y. Y.; Jackson, T. N.; Schlom, D. G. *Appl. Phys. Lett.* **1997**, *71*, 3853–3855.
8. Deeg, O.; Kirsch, P.; Pauluth, D.; Bäuerle, P. *Chem. Commun.* **2002**, 2762–2763.
9. Yu, Z. N.; Tu, H. L.; Wan, X. H.; Chen, Z. F.; Zhou, Q. F. *Mol. Cryst. Liq. Cryst.* **2003**, *391*, 41–45.
10. Sultana, N. H.; Kelly, S. M.; Mansoor, B.; O'Neill, N. *Liq. Cryst.* **2007**, *34*, 1307–1316.
11. Sidorov, V.; Douglas, T.; Dzekunov, S. M.; Abdallah, D.; Ghebremariam, B.; Roepe, P. D.; Matile, S. *Chem. Commun.* **1999**, 1429–1430.
12. Baumeister, B.; Matile, S. *Chem. Commun.* **2000**, 913–914.
13. Singh, D. L.; Jayasuriya, H.; Dewey, R.; Polishook, J. D.; Dombrowski, A. W.; Zink, D. L.; Guan, Z.; Collado, J.; Platas, G.; Pelaez, F.; Felock, D. J.; Hazuda, D. J. *J. Ind. Micro. Biotechnol.* **2003**, *30*, 721–731.
14. Baumeister, B.; Sakai, N.; Matile, S. *Angew. Chem., Int. Ed.* **2000**, *39*, 1955–1958.
15. Yin, H.; Lee, G.-I.; Sedey, K. A.; Kutzki, O.; Park, H. S.; Orner, B. P.; Ernst, J. T.; Wang, H.-G.; Sebti, S. M.; Hamilton, A. D. *J. Am. Chem. Soc.* **2005**, *127*, 10191–10196.
16. Yamaguchi, I.; Goto, K.; Sato, M. *Tetrahedron* **2009**, *65*, 3645–3652.
17. Robert, F.; Winum, J.-Y.; Sakai, N.; Gerard, D.; Matile, S. *Org. Lett.* **2000**, *2*, 37–39.
18. Nijegorodou, N.; Downey, W. S.; Danailov, M. B. *Spectrochim. Acta, Part A* **2000**, *56*, 783–795.
19. Zhang, X.; Shetty, A. S.; Jenekhe, S. A. *Macromolecules* **1999**, *32*, 7422–7429.
20. Lightowler, S.; Hird, M. *Chem. Mater.* **2004**, *16*, 3963–3971.